AEROSTRUCTURAL DESIGN OF A MEDIUM-ALTITUDE MEDIUM-ENDURANCE FIXED WING UAV

PEDRO M. CARDOSO[1], ANDRÉ C. MARTA[1] AND NUNO B. MATOS[2]

[1] IDMEC, Instituto Superior Técnico, Universidade de Lisboa,
Av. Rovisco Pais 1, 1049-001 Lisboa, Portugal
{pedro.marques.cardoso,andre.marta}@tecnico.ulisboa.pt, https://mdo.tecnico.ulisboa.pt

[2] Research and Development, TEKEVER UAS,
Rua das Minas 2, 2500-750 Caldas da Rainha, Portugal
nuno.matos@tekever.pt, https://tekever.com/

Key words: multidisciplinary optimization, aircraft design, adjoint method, high-fidelity methods, free-form deformation, composite materials

Summary. The UAV market is currently very populated, driving the manufacturers to design more efficient solutions to obtain a competitive edge. A cost-effective approach is to improve existing products using new technologies and design tools. This work addresses the desire of a UAV manufacturer to develop a growth version of an existing Medium-Altitude Medium-Endurance (MAME) Unmanned Aerial Vehicle (UAV). To that end, the aerostructural optimization of the wing is performed using coupled high-fidelity Computational Fluid Dynamics (CFD) and Computational Structural Dynamics (CSD). Gradient-based optimization fed with derivatives of functions of interest computed using the adjoint method are used for computational efficiency. The coupled problem is posed in the aerostructural optimization framework, targeting for maximum aircraft range, being the solution a result of the concurrent discipline analyses. The set of design variables include wing twist distribution, using the free-form deformation approach, material thicknesses and carbon fibre orientations. The optimized wing geometry exhibits a gain of 5% in aircraft range, with 2% better aerodynamic efficiency (L/D) and 63% wing weight reduction. The impact of multilayer composite manufacturing constraints, namely adjacency of ply angles in neighbouring regions and the orthogonality between ply angles, was found not to be significant. The studies identified weaknesses of the baseline wing and provided meaningful engineering insights for the next generation MAME UAV design.

1 INTRODUCTION

The development of fixed-wing UAVs has advanced significantly since the 20th century. Initially driven for military applications, these technologies are becoming increasingly prevalent in a variety of civilian uses [1]. In 2023, the drone market was evaluated in 34 billion US$, with 21% market share for fixed-wing UAVs. Given the projected Compound Annual Growth Rate (CAGR) between 8.3 and 17.2% [2], the competition among manufacturers is fierce.

The goal of this work is to assist in the development of a second-generation TEKEVER AR5 (Figure 1) model to increase its value proposition in the current Medium-Altitude Medium-Endurance (MAME) fixed-wing UAV market. This model can perform missions such as search

Figure 1: TEKEVER AR5 (source: TEKEVER UAS)

and rescue, maritime surveillance, and maritime patrol, benefiting from reasonable endurance, and reduced operating costs [3]. Table 1 contains its main characteristics.

Table 1: TEKEVER AR5 characteristics [3]

Cruise speed	Cruise altitude	Payload	Wing span	Wing area	Length	Endurance	Comms range	Recovery and launch
100 km/h	1000 ft	50 kg	7.3 m	4.36 m^2	4 m	20 h	unlimited	unprepared airstrip

The objective is to re-design its main wing for improved aerodynamic and structural performance. Since the wing is a flexible, elastic structure, whose jig (unloaded) shape differs significantly from the in-flight (aerodynamically loaded) shape, due to significant fluid-structure interaction, a high-fidelity coupled aerostructural design tool is sought.

2 AEROSTRUCTURAL DESIGN FRAMEWORK

The aerostructural design framework used is MACH-Aero, developed by the Multidisciplinary Design Optimization (MDO) Laboratory at the University of Michigan [4]. It includes three main stages, as depicted in Figure 2.
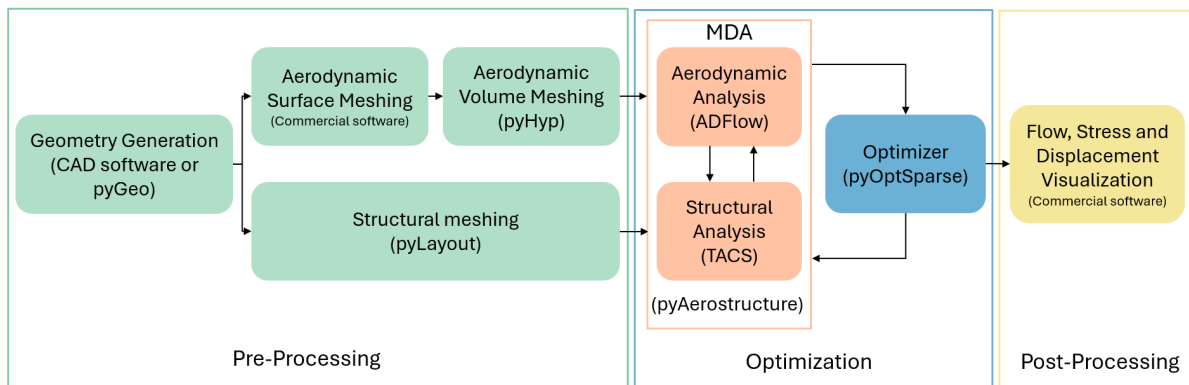

Figure 2: Aerostructural design framework

2.1 Pre-processing stage

The baseline geometry definition is performed using commercial Computer Aided Design (CAD) software or custom tools like `pyGeo`. Free-Form Deformation (FFD), a deformation method, is then used to efficiently modify the baseline geometry during optimization without requiring further CAD usage [5]. FFD boxes defined by control points surrounding the wing surface are shown in Figure 3. Although each FFD point can move individually, `pyGeo` can aggregate them into global variables, such as twist and chord distributions, thus reducing the number of design variables.
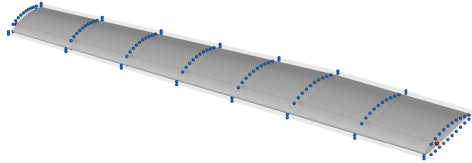

Figure 3: Free form deformation (FFD) box

Based on the geometry CAD description, the aerodynamic surface mesh is then created, followed by the generation of the volume mesh (Figure 4a) using `pyHyp`, which also applies the boundary conditions [4]. The first layer height was prescribed to guarantee a y+ close to unity as required by the Spalart-Allmaras turbulence model employed. A mesh refinement study concluded that 200,000 elements were sufficient, considering the trade-off between accuracy and performance, with 0.5% difference in lift and drag in relation to the most refined mesh studied. The volume domain size extended for 20 chords, which kept the errors in lift and drag under 1%.

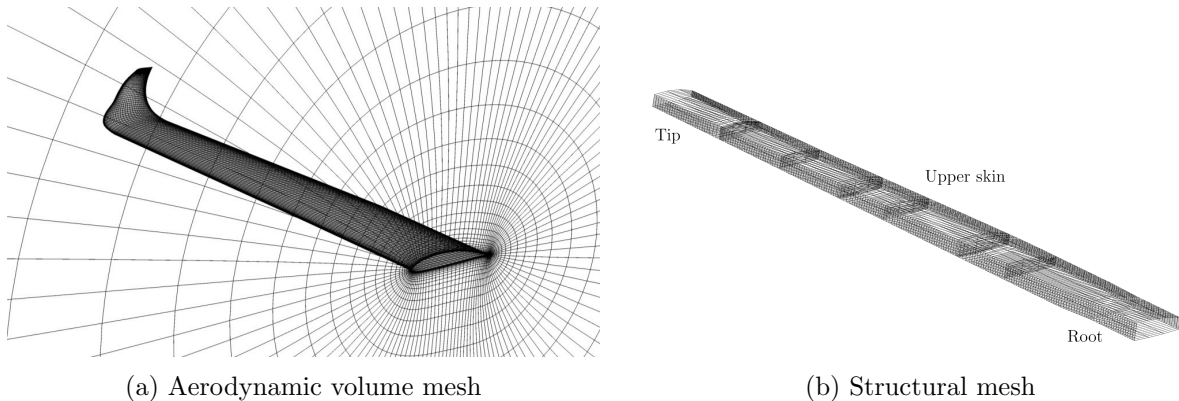(a) Aerodynamic volume mesh

(b) Structural mesh

Figure 4: Computational meshes of TEKEVER AR5 wing

The structural mesh is generated with `pyLayout`, which is a module tailored for the automated creation of parametric structures for wings. By describing the structural layout, it constructs a finite-element model for the wingbox, as shown in Figure 4b. Since these wing parts are thin and made of fibre-reinforced composite materials, bilinear, 4-node, 2-D shell elements were used. From a mesh convergence study monitoring the failure index, a mesh with 60,000 DoF was

selected, which presents an 9% error, but were aligned with the computational power available.

2.2 Optimization stage

The Multidisciplinary Feasible (MDF) MDO architecture is selected for its simplicity and accuracy at the optimizer level [6]. MDF works as single discipline optimization, where the evaluation of the disciplines is done in a coupled fashion by means of a Multidisciplinary Analysis (MDA). Besides taking advantage of already well-developed, discipline-specific solvers, this approach also has an advantage of yielding feasible intermediate solutions in case of optimizer failure [7]. The aerodynamic discipline is solved using `ADFLOW` [8] and the structural discipline is solved using `TACS` [9].

`ADFLOW` uses a finite-volume formulation to solve the steady compressible RANS equations with the Spalart-Allmaras turbulence model. The flow properties are computed using the International Standard Atmosphere for the prescribed altitude. Central finite-differences with JST scalar dissipation is used for the spatial discretization. It employs characteristic time-stepping with an approximate Newton method, aided by van Leer-Lee-Roe preconditioner that has been shown to improve accuracy and convergence for low Mach number. The L2-norm of the residual is converged when a reduction of 10^{-6} is achieved. All other aerodynamic solver parameters kept their default value [8].

`TACS` uses a finite-element formulation to solve the generalized Hooke's Law [10]. For thin structures, like wing skins, 4th order, 2-D shell elements are used. The material properties are assumed orthotropic, with the fibres parallel within a ply, allowing for the use of the rule of mixtures [11]. The failure criterion for the composite material is the Tsai-Wu [12].

The disciplines are coupled using `pyAerostructure`, which captures the interactions between aerodynamic forces and structural displacements. The MDA is converged using Gauss-Seidel [13], a fixed-point method in which each discipline analysis is run using the most recent output from the other disciplines until a consistent set of state variables is returned. Since each component of the new iterate depends on all previously computed components, the updates cannot be done simultaneously but it exhibits better stability when compared to the Jacobi method in aircraft design [14]. The MDA convergence tolerance was set to 10^{-5}.

The fluid-structure interaction is achieved by exchanging aerodynamic loads and structural displacements between the discipline domains at their interface. Typically, the aerodynamic and structural nodes at the body (wing) surface differ, mainly due to the different mesh resolutions, so the Rigid Link Transfer (RLT) [15] displacement transfer method is used, as illustrated in Figure 5. The RLT starts by identifying the closest point on the structural mesh for each aerodynamic surface node, defining a link vector r. Subsequently, the structural FEM shape functions are employed to interpolate the translation and rotation of the link's base, computing the aerodynamic node displacement u_A based on the rigid translation u_t and rotation u_r of the link as

$$\{u_A\} = \{u_t\} + \{u_r\} \times \{r\}. \tag{1}$$

Since the second term is a linearized approximation, this method is limited to small rotations. An initial structural-aerodynamic damping factor of 0.1 is used to prevent negative volumes, failed aerodynamic meshes, from occurring due to poorly converged solutions. The RLT method has been seamlessly integrated into the `TACS` solver with gradients computed analytically [13]. As for the aerodynamic load transfer, the method of virtual work is used to determine the
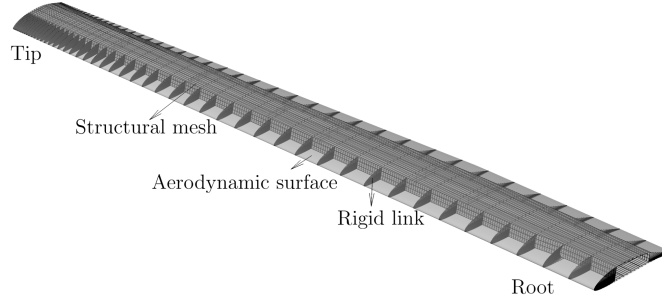
Figure 5: Overlay of the structural mesh, aerodynamic surface and rigid links

structural nodal forces [16], given by the integration on the aerodynamic surface as

$$\delta W = \int_{S_A} p\mathbf{n} \cdot \delta\mathbf{u}_A \, dS = \int_{S_A} p\mathbf{n} \cdot \delta\mathbf{u}_S - p\mathbf{n} \cdot (\mathbf{r} \times \delta\theta_S) \, dS \,, \tag{2}$$

where p is the surface pressure, $\mathbf{n}$ is the normal defined on the aerodynamic surface mesh S_A.

During the aerostructural optimization process, changes to the external shape of the wing arise from design adjustments and structural deformations. To address these changes in surface geometry, the CFD mesh is updated using an Inverse-Distance Weighting method (IDW), in which the displacement of a volume node is computed as a weighted average of the boundary node displacements, the weight being the inverse of the distance between the volume and the boundary nodes [17].

The optimization process, driven by `pyOptSparse`, tunes the Design Variables (DV) to improve the performance metric (objective function), while adhering to specified requirements (constraints). The optimization algorithm chosen is the SLSQP, which has been shown to outperform other methods in aerodynamic and aerostructural problems [18]. Being a gradient-based algorithm, it efficiently navigates high dimensional design spaces, provided both the objective and constraint functions are smooth [19].

The sensitivity analysis, required for the search direction evaluation, is efficiently and accurately performed using the adjoint method since there are more design variables than metric functions [20]. The coupled system of adjoint equations is treated as a single, unified problem, directly addressing the interdependencies between different disciplines by solving the entire set of coupled adjoint equations simultaneously,

$$\begin{bmatrix} \frac{\partial R_A}{\partial u_A} & \frac{\partial R_A}{\partial u_S} \\ \frac{\partial R_S}{\partial u_A} & \frac{\partial R_S}{\partial u_S} \end{bmatrix} \begin{Bmatrix} \lambda_A \\ \lambda_S \end{Bmatrix} = \begin{Bmatrix} \frac{\partial J}{\partial u_A} \\ \frac{\partial J}{\partial u_S} \end{Bmatrix} \,, \tag{3}$$

where the governing set of nonlinear equations are expressed as $R(u, x) = 0$, where u represents the state variables, x the design variables and λ the adjoint variables, for each discipline, either aerodynamics (subscript A) and structures (subscript S). This ensures that all disciplinary interactions are accounted for in a cohesive manner, leading to more accurate sensitivity analysis and faster convergence [21]. The adjoint solver is converged using the Krylov subspace approach, with a tolerance of 10^{-5}. The gradient of the objective (or constraint) function J with respect to the design variables x is then given by

$$\frac{dJ}{dx} = \frac{\partial J}{\partial x} - \lambda_A^T \frac{\partial R_A}{\partial x} - \lambda_S^T \frac{\partial R_S}{\partial x} \,, \tag{4}$$

with no dependence on u, allowing the derivative to be taken in each optimizer iteration without the need of solving the PDE [22].

3   TEKEVER AR5 MULTIDISCIPLINARY ANALYSIS

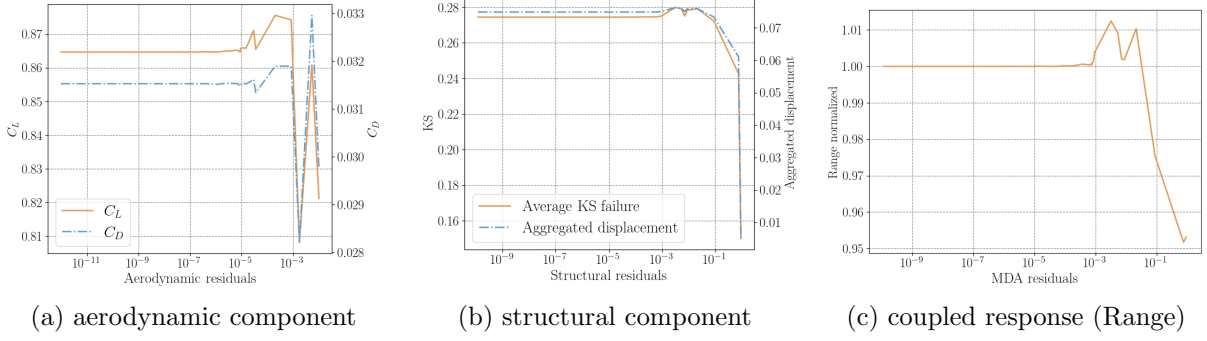The effect of the MDA convergence was studied, with the results summarized in Figure 6. It

(a) aerodynamic component

(b) structural component

(c) coupled response (Range)

Figure 6: Effect of MDA residual convergence tolerance

is possible to confirm the suitability of the chosen value of 10^{-5}, that sits in the advised range from 10^{-6} to 10^{-3} [21].

The lift coefficient C_L as a function of angle-of-attack α of the simplified AR5 wing without the winglet is shown in Figure 7a for both the rigid model (aerodynamic analysis using the wing jig shape) and the elastic model (aerostructural analysis). The wing deformation in the aerostructural analysis results in a change of its aerodynamic shape and incidence angle, causing an increase in lift for high angles-of-attack, delaying and smoothing the stall condition. This result reveals that the aerostructural coupling is significant and must accounted for in the wing design. Additionally, it also highlights that there is an adverse bending-twist behavior in the baseline wing.

The aerodynamic shape comparison between the two models is illustrated in Figure 7b, reinforcing the strong fluid-structure interaction.
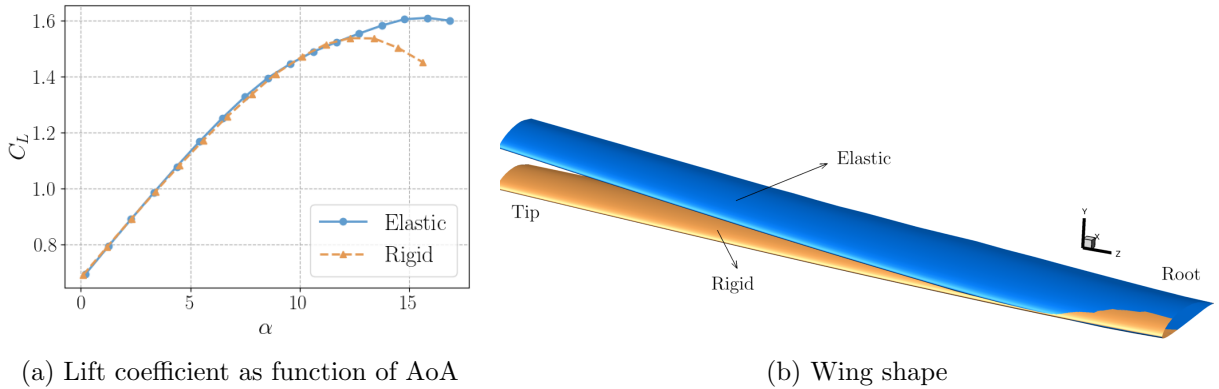
(a) Lift coefficient as function of AoA

(b) Wing shape

Figure 7: Comparison between rigid and elastic wing model

4 TEKEVER AR5 MULTIDISCIPLINARY OPTIMIZATION

4.1 Performance metrics, design variables and constraints

The aerostructural optimization targets the maximization of the aircraft range R defined by the Breguet equation,

$$R = \frac{C_L}{C_D} \frac{\eta}{sfc \cdot g} \ln\left(\frac{W_0}{W_f}\right) , \qquad (5)$$

where the lift C_L and drag C_D coefficients depend on the aerodynamic performance, and the initial W_0 and final W_f weight depend on the structural performance. The aircraft velocity is prescribed by the flight operating condition, the engine efficiency η and specific fuel consumption sfc are frozen given the propulsion system, and g is the gravitational acceleration.

The wing design variables, that allow for the definition of its shape and structure, are summarized in Table 2.

Table 2: Design variables

Design variable	Description	Quantity	Lower bound	Upper bound	Units
α	angle of attack	1	-4	20	°
γ	twist distribution	7	-15	15	°
θ_1/θ_2	fibre angle	2N	0	90	°
t	material thickness	N	0.01	0.1	m

Notice that the twist distribution is a function of the wing spanwise coordinate, being defined by splines using seven control airfoil sections each (see Figure 3). The fibre angles and material thickness are defined for each block i of the N blocks presented in Figure 8.
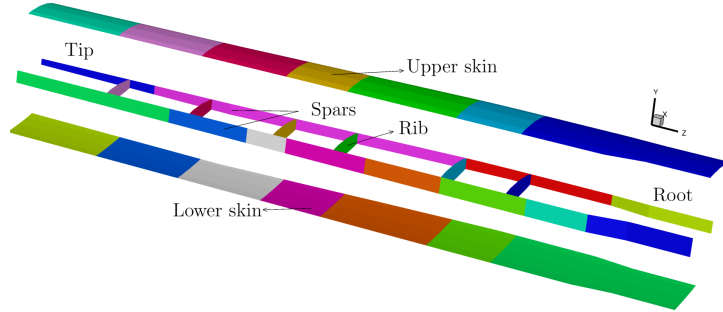

Figure 8: Wing structural design variables by blocks

The design must satisfy five requirements, included in the form of constraints in the optimization: i) the trimming of the aircraft implies that the lift generated must match the UAV weight at level flight, $L = W$; the structure must not fail under a 2-g manoeuvre, $KS(failure) \leq n(2g)$; iii) adjacency constraints to keep the difference in each design block thickness under a maximum threshold, $|t_i - t_{i+1}| \leq \Delta_{max}$; iv) composite ply angle continuity among consecutive blocks for manufacturability, $\theta_{1,i} = \theta_{1,i+1}$ and $\theta_{2,i} = \theta_{2,i+1}$; and v) orthogonality between plies for manufacturability to allow the use of carbon fibre cloths with weaving pattern, $|\theta_1 - \theta_2| = 90°$.

The wing aerostructural optimization problem is then posed in standard form as

$$
\begin{aligned}
\text{maximize} \quad & R \\
\text{with respect to} \quad & \alpha, \gamma, \theta_{1,i}, \theta_{2,i}, t_i \\
\text{subject to} \quad & L = W \\
& KS(\text{failure}) \leq n(2g) \\
& |t_i - t_{i+1}| \leq \Delta_{\max} \\
& \theta_{1,i} = \theta_{1,i+1} \\
& \theta_{2,i} = \theta_{2,i+1} \\
& |\theta_1 - \theta_2| = 90°
\end{aligned}
\tag{6}
$$

4.1.1 Optimal wing design without manufacturing constraints

Starting from the simplified TEKEVER AR5 wing design without winglet, a first optimization was done without the two manufacturability constraints (iv) and (v). Overall, it achieved 1.9% increase in aerodynamic efficiency and a 5% increase in range.

Figure 9 shows the convergence history of five key parameters in 275 iterations. During the initial iterations, it is clear the need to operate at higher angle-of-attack for trimming (Fig.9b), the reduction of (induced) drag (Fig.9c) by controlling the lift distribution (Fig.10a) with the twist angle (Fig.10b), and the search for a lighter structure (Fig.9d) while avoiding structural failure (Fig.9e).
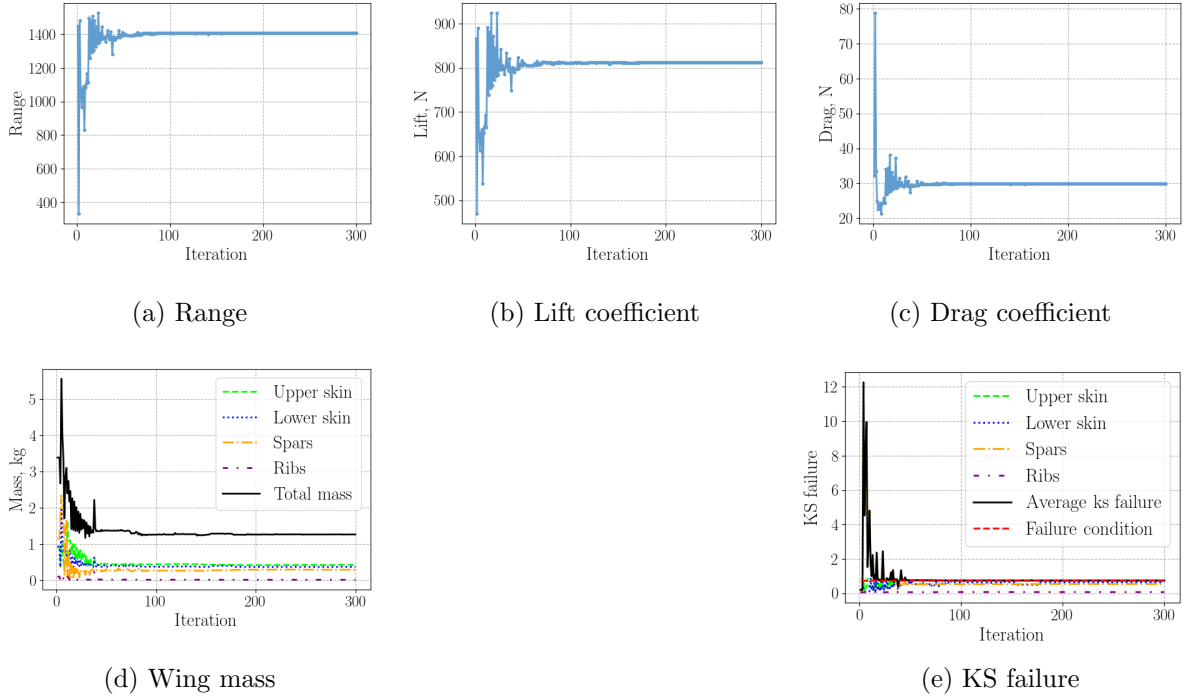

(a) Range

(b) Lift coefficient

(c) Drag coefficient

(d) Wing mass

(e) KS failure

Figure 9: Optimization history of key parameters

The optimal twist and lift distributions are shown in Figure 10. As expected, the optimizer did not to converge for the ideal aerodynamic solution (elliptical lift distribution) but rather increased the lift produced in the inner portion of the wing and reduced it closer to the tip, contributing to a more beneficial structural loading (less bending moment, thus lighter structure) and an overall better coupled aerostructural solution.
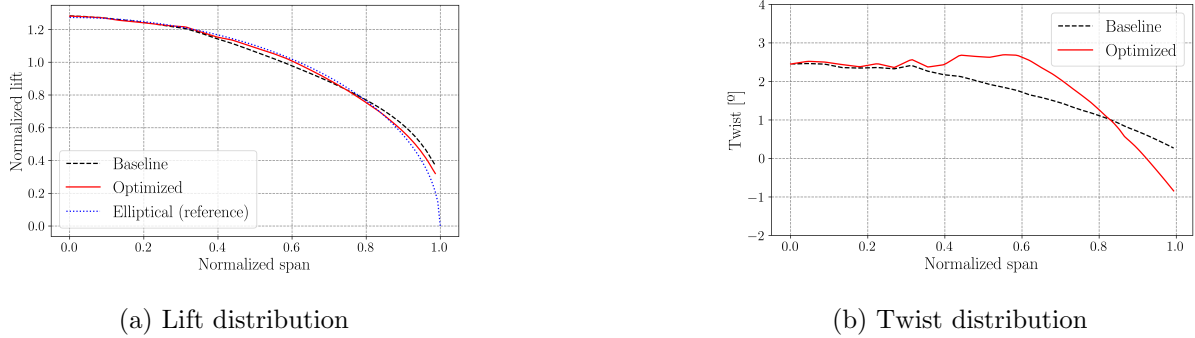

(a) Lift distribution

(b) Twist distribution

Figure 10: Aerodynamic spanwise distributions

This case led to a drastic improvement of the structural efficiency, as attested by the increase in the KS index failure (Fig.9e). As a consequence, a 63% wing weight reduction occurred due to the significant thinning of panels observed in Figure 11, particularly at the front spar and lower skin panels.

Referring to Figure 12, the optimized wingbox has more regions with a higher failure index, meaning that it is working closer to failure due to the overall thickness decrease, highlighting the baseline wingbox structural oversizing.

The ply angle distribution between the blocks is shown in Figure 13. It can be verified that, when the optimizer is given full freedom without the manufacturing constraints, the solution is non-monotonic distribution, which would make manufacturing difficult. Furthermore, the fact that the angle between plies is not 90 degrees makes it impossible to use standard interwoven carbon fiber, increasing the cost of wing manufacturing.

4.1.2 Effect of manufacturing constraints

To address the issues described, the manufacturing constraints of adjacency ply angles (iv) and orthogonality (v) were added. Figure 14 demonstrates that the new optimal solution is now feasible in terms of manufacturing, being this solution much easier to implement with its orthogonal plies and consistency in ply angles.

With these additional constraints, the aircraft range increased 4.7% compared to the baseline, representing a slight loss relative to the previous non-manufacturing constrained case (-0.3%).

5 CONCLUSIONS

High-fidelity MDO has been demonstrated as a powerful tool for aerostructural wing design. Gains in aircraft range of +5% were obtained, resulting from a combination of +2% improvement in aerodynamic efficiency by tweaking the wing twist and a substantial -63% wing weight

reduction by adjusting the shell thickness and the fibre angles of the composite plies. The impact of multilayer composite manufacturing constraints, namely adjacency of ply angles in neighbouring regions and the orthogonality between ply angles, was found not to be significant.
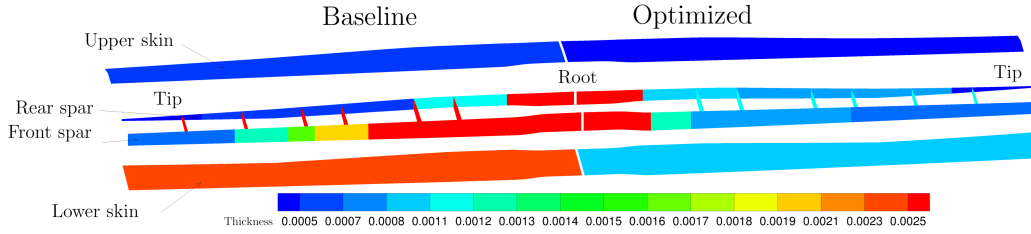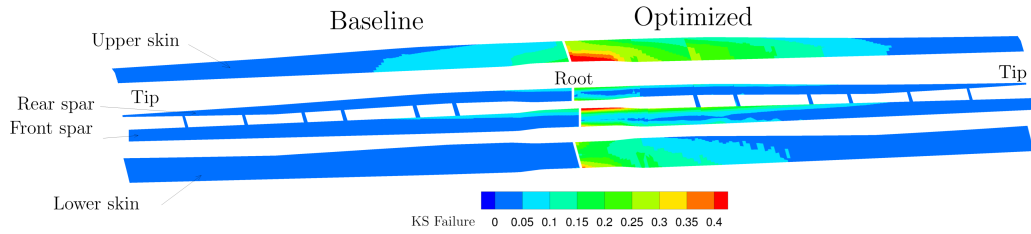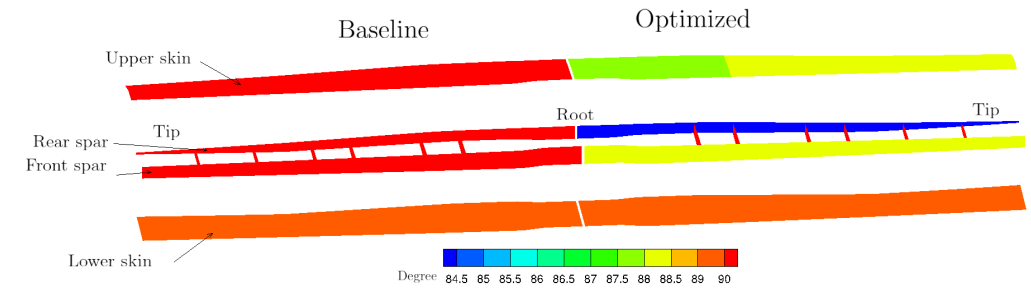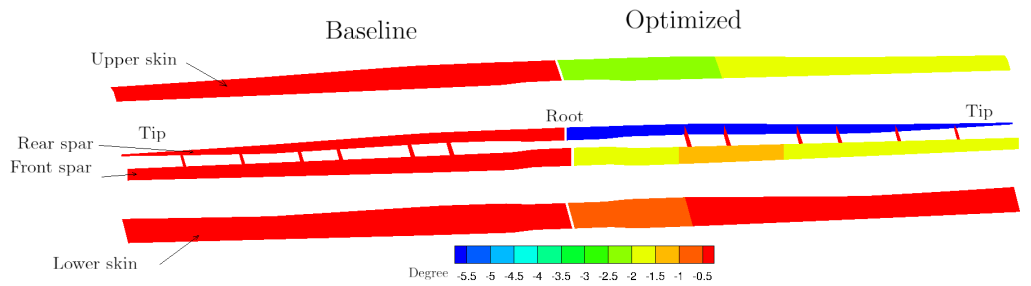

Figure 11: Thickness distribution

Figure 12: KS failure index

(a) Angle θ_1

(b) Angle θ_2

Figure 14: Optimal distribution of ply angles with manufacturing constraints
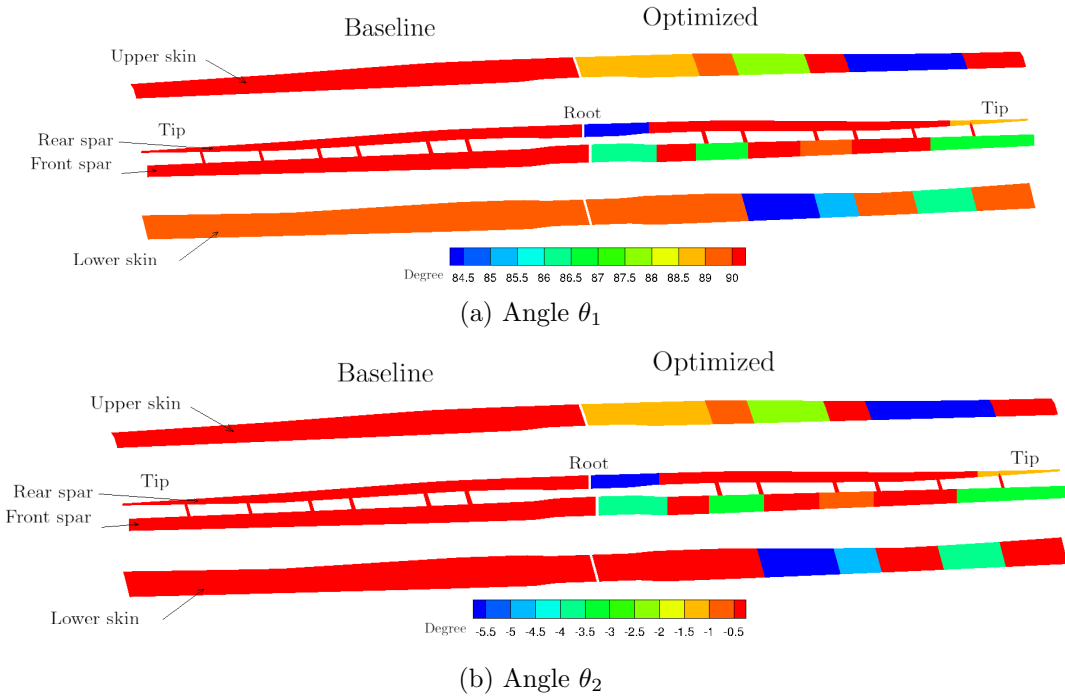
(a) Angle θ_1

(b) Angle θ_2

Figure 13: Optimal distribution of ply angles without manufacturing constraints

6 Acknowledgments

REFERENCES

[1] P. Höhrová, J. Soviar, and W. Sroka, "Market Analysis of Drones for Civil Use," *LOGI – Scientific Journal on Transport and Logistics*, vol. 14, no. 1, 2023. doi:10.2478/logi-2023-0006.

[2] Grand View Research, "Commercial drone market size, share & trends analysis report and segment forecasts, 2023-2030." `https://www.grandviewresearch.com/industry-analysis/global-commercial-drones-market`, 2023. (accessed on 2023-09-10).

[3] TEKEVER UAS, "Tekever AR5." `https://www.tekever.com/models/ar5/`, 2023. (accessed on 2023-12-03).

[4] MDO Lab of University of Michigan, "MACH-Aero Framework." `https://mdolab-mach-aero.readthedocs-hosted.com`, 2023. (accessed on 2024-04-03).

[5] T. W. Sederberg and S. R. Parry, "Free-form deformation of solid geometric models," in *SIGGRAPH '86: Proceedings of the 13th Annual Conference on Computer Graphics and Interactive Techniques*, (New York, USA), Aug. 1986. doi:10.1145/15922.15903.

[6] A. C. Gray and J. R. Martins, "Geometrically nonlinear high-fidelity aerostructural optimization for highly flexible wings," in *AIAA Scitech 2021 Forum*, (Virtual event), Jan. 2021. doi:10.2514/6.2021-0283.

[7] R. Perez, H. Liu, and K. Behdinan, "Evaluation of multidisciplinary optimization approaches for aircraft conceptual design," in *10th AIAA/ISSMO multidisciplinary analysis and optimization conference*, (Albany, USA), Aug. 2004. doi:10.2514/6.2004-4537.

[8] MDO Lab of University of Michigan, "ADFlow Documentation." `https://mdolab-adflow.readthedocs-hosted.com`, 2024. (accessed on 2024-04-03).

[9] G. J. Kennedy and J. R. Martins, "A parallel finite-element framework for large-scale gradient-based design optimization of high-performance structures," *Finite Elements in Analysis and Design*, vol. 87, 2014. doi:10.1016/j.finel.2014.04.011.

[10] J. N. Reddy, *Mechanics of Laminated Composite Plates and Shells: Theory and Analysis*. CRC Press, 2nd ed., 2003. doi:10.1201/b12409.

[11] D. R. Askeland, P. P. Fulay, and W. J. Wright, *The Science and Engineering of Materials*. Cengage Learning, 6th ed., 2010. ISBN:9780495296027.

[12] A. Khani, S. T. IJsselmuiden, M. M. Abdalla, and Z. Gürdal, "Design of variable stiffness panels for maximum strength using lamination parameters," *Composites Part B Engineering*, vol. 42, no. 3, 2011. doi:10.1016/j.compositesb.2010.11.005.

[13] A. C. Gray, C. Riso, E. Jonsson, J. R. R. A. Martins, and C. E. S. Cesnik, "High-fidelity aerostructural optimization with a geometrically nonlinear flutter constraint," *AIAA Journal*, vol. 61, no. 6, 2023. doi:10.2514/1.J062127.

[14] M. Zimmnau, F. Schültke, and E. Stumpf, "UNICADO: multidisciplinary analysis in conceptual aircraft design," *CEAS Aeronautical Journal*, vol. 14, 2023. doi:10.1007/s13272-022-00620-3.

[15] S. Brown, "Displacement extrapolations for CFD+CSM aeroelastic analysis," in *Proceedings of the 38th Structures, Structural Dynamics, and Materials Conference*, (Kissimmee, USA), Apr. 1997. doi:10.2514/6.1997-1090.

[16] G. J. Kennedy and J. R. R. A. Martins, "Parallel solution methods for aerostructural analysis and design optimization," in *Proceedings of the 13th AIAA/ISSMO Multidisciplinary Analysis Optimization Conference*, (Fort Worth, USA), Sept. 2010. doi:10.2514/6.2010-9308.

[17] N. Secco, G. K. W. Kenway, P. He, C. A. Mader, and J. R. R. A. Martins, "Efficient mesh generation and deformation for aerodynamic shape optimization," *AIAA Journal*, vol. 59, no. 4, 2021. doi:10.2514/1.J059491.

[18] Z. Lyu, Z. Xu, and J. R. R. A. Martins, "Benchmarking optimization algorithms for wing aerodynamic design optimization," in *Proceedings of the 8th International Conference on Computational Fluid Dynamics*, (Chengdu, China), July 2014. ICCFD8-2014-0203.

[19] N. Wu, C. A. Mader, and J. R. R. A. Martins, "A gradient-based sequential multifidelity approach to multidisciplinary design optimization," *Structural and Multidisciplinary Optimization*, vol. 65, no. 131, 2022. doi:10.1007/s00158-022-03204-1.

[20] J. R. R. A. Martins and G. Kennedy, "Enabling large-scale multidisciplinary design optimization through adjoint sensitivity analysis," *Structural and Multidisciplinary Optimization*, vol. 64, 2021. 10.1007/s00158-021-03067-y.

[21] G. K. W. Kenway, G. J. Kennedy, and J. R. R. A. Martins, "Scalable parallel approach for high-fidelity steady-state aeroelastic analysis and adjoint derivative computations," *AIAA Journal*, vol. 52, no. 5, 2014. doi:10.2514/1.J052255.

[22] J. R. R. A. Martins and A. Ning, *Engineering Design Optimization*. Cambridge University Press, 2022. doi:10.1017/9781108980647.